MCM TRIALS WITH BIOSONAR SYSTEM

Yan Pailhas Heriot Watt University, Edinburgh, UK
Chris Capus Hydrason Solutions Ltd, Edinburgh, UK
Keith Brown Heriot Watt University, Edinburgh, UK

1 INTRODUCTION

In this paper we present the results of MCM trials using a Biosonar system mounted on the AUV (autonomous underwater vehicle) REMUS 100. The trials were run in Lochearnhead in Scotland. Two mine-like objects were put on the seafloor. The first one was a aluminium cylinder (150 cm long and 40 cm diameter) and the second object was a truncated cone shaped aluminium shell (Manta mine like target). The REMUS 100 was equipped with a standard Marine Sonics sidescan sonar. The Biosonar payload was in a side-looking configuration. Data were gathered using both sensors simultaneously. A first set of runs covered the delimited search area using a lawnmower pattern. The AUV then returned to the interesting detected objects and reacquired them following a dolphin-like spiral to obtain further data giving a range of views of the objects. The data supplied have demonstrated that the wideband sonar system is very effective at identifying seafloor objects.

2 OBJECT IDENTIFICATION VIA BROADBAND ECHOES

At first active sonars were used as a range measurement tool. By measuring the time t between when the system sends the pulse and when the echo arrives, and knowing the sound speed c in water, one can compute the range r between the sonar and the target by the simple equation: $r = ct/2$.

However the understanding of the full echo structure requires the resolution of the wave propagation equation. This equation has been solved for simple cases such as spheres, cylinders (Refs. [1, 2]), spherical shells in Ref. [3] and cylindrical shells in Ref. [4]. Analytical solutions are not available for objects with more complex shape and numerical simulations or models are needed at this point.

The echo is the result of the interaction of the incoming acoustic wave with the target of interest. Echoes are characterised by multiple returns from the target. In the Fourier domain these multiple returns interfere and create notches in the echo spectra. In Ref. [5] Pailhas and al. proved that the localisation of the notches are stable features for identification. The feature extraction can be computed as followed:

Let F be the spectrum of the backscattered echo and let $\{\omega_n\}_{n\in[1,\ N]}$ be the location in frequency of the notches. We associate ΔF to F by:

$$\Delta F(\omega) = \sum_{n=1}^{N} \delta(\omega - \omega_n) * G_\sigma(\omega) \tag{1}$$

where δ represents the Dirac function and G_σ is the centered Gauss function with a variance of σ. The ΔF function is an irregular Gauss comb where the peaks represent the notch locations.

A metric can be associated to this space and the distance between two elements ΔF and ΔG can be defined by:

$$d(\Delta F, \Delta G) = \left(\int_0^{+\infty} |\Delta F(\omega) - \Delta G(\omega)|^2 d\omega \right)^{1/2} \quad (2)$$

To test the performance of the dolphin-inspired sonar an experiment to identify six man-made targets was set up in a test tank. The six man-made targets are of similar dimensions but different shapes and materials. The classification was performed using the distance metric Eq. (2) in a controlled environment [5]. The correct identification rate was greater than 90%. Table 1 shows the confusion matrix of the broadband classifier using the distance defined by Eq. (2) and the two bio-mimetic pulses DC1 and DC6. The performance in correct identification of objects that have very similar amplitude returns illustrates the strength of the approach.

DC1 & DC6	cone	cone 8° tilted	pipe	tube	rocket head	brick (length)	brick (width)
cone	**0.50**	0.21	0	0	0	0	0
cone 8° tilted	0.29	**0.59**	0.05	0	0	0	0
pipe	0.12	0	**0.81**	0.06	0	0	0
tube	0.09	0.12	0	**0.94**	0	0	0
rocket head	0	0.08	0.14	0	**1.00**	0	0
brick (long)	0	0	0	0	0	**1.00**	0
brick (large)	0	0	0	0	0	0	**1.00**

Table 1: Confusion matrix for the fusion system of the two classifiers relative to the two bio-mimetic pulses DC1 and DC6.

The RST (resonance scattering theory) predicts strong interferences in the frequency range $ka \in [10,\ 50]$ where $k = \frac{2\pi f}{c}$ is the wavenumber, f the frequency, c the speed of sound in water and a is a key target dimension (e.g. radius for a cylinder or a sphere) [6]. This simply stipulates that the distance between two principal scatterers in the target should be larger that one wavelength to create measurable interferences and smaller than ten wavelengths for the interferences to be trackable.

Our transducers cover a similar frequency band to that used by dolphins: from 30 kHz to 130 kHz. According to the RST, this frequency band is optimal to characterise objects with a key target dimension included between 2 cm and 40 cm. We note that these dimensions match with the prey of dolphins. This argument indicates that even lower frequency systems will be useful for dealing with larger objects.

3 OBJECT IDENTIFICATION FROM AN AUV

A prototype dolphin-inspired sonar was built and attached to a REMUS-100 AUV. The bio-inspired sonar was mounted in a side-looking configuration to facilitate gathering of collocated sidescan data with that of the vehicle's standard Marinesonics sonar at 900 kHz operating frequency.

A series of trials to validate the capacity of the dolphin inspired sonar for object recognition in a real environment operating from this reliable and commonly used autonomous vehicle were performed. A set of spherical targets were put together for these trials. Spheres provide a good reference target because of their rotational symmetries. The target itself will give a similar echo response at any angle of view, range or altitude. All the targets have a similar diameter (between 28 cm and 38 cm) and were made using different materials: stainless steel, concrete or plastic. Using conventional imaging sonar it is impossible to identify one target from another. The experiments were performed on a relatively flat region (at a depth of around 38 metres) giving good conditions for multi-aspect survey of the full target set.

In the experiment we aim to demonstrate the capability to distinguish targets with the same shape and similar dimensions but constructed from different materials or to distinguish a solid target from

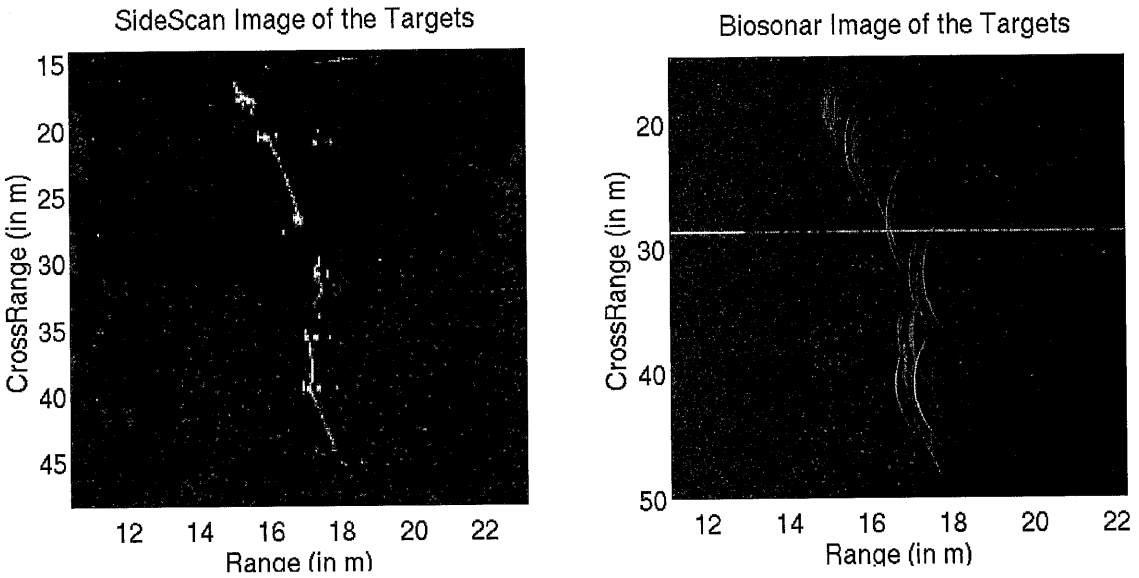

Figure 1: Spherical targets with roughly the same dimension (Ø: around 30 cm) but built with different materials (plastic, aluminium or concrete) have been put on the seafloor. The figure displays a close up of the targets using sidescan (on the left), and using BioSonar (on the right). All the targets appear very similar in the sidescan image and are impossible to differentiate. However in the BioSonar image, the characteristic resonances of the different targets are clear which make identification possible.

a hollow target. These are fundamental capabilities for the recognition of manmade targets amongst natural clutter objects.

Figure 1 shows close ups over the target set for both sensors. The registered sidescan image is displayed on the left, and the bio-inspired image on the right. The bio-inspired images are produced for visualisation purposes only from the envelope of the matched filtered echo. Object identification is performed from the individual return signals, as explained in the following paragraphs. Note that the wide beamwidth of the system, leads to the target responses tracing arcs through the data, in similar fashion to raw SAS. The sidescan gives quite high resolution images allowing us to clearly locate each of the targets and gives a good response along the line connecting them (8mm braided polyethylene). Note that in the sidescan image, it is impossible to identify one target from another. Multiple responses at broadside do give some indication that certain targets are resonant. Whilst precise location is more complicated working from the wideband returns, the resonances are more easily picked up in the parallel arcs associated with these targets.

Here we describe an identification method using a time-domain Gaussian mixture model to represent the echo of the large steel sphere. Note that the time domain refers to the matched filtered echo. A mixture of 4 gaussians has been chosen to model the envelope of the backscattered echo of the big steel sphere. The time domain methods suffer some limitations. In particular the match filtering in the time domain compresses the broadband pulses and tends to suppress the frequency dependance of the echo components (especially the secondary echoes) and spread the envelope. However the bandwidth used by the bio-inspired sonar provides a relatively clear echo and almost linear echo in the frequency domain. For this reason the resulting match filtered echo exhibits strong and sharp specular and secondary responses for the targets of interest. Figure 2 displays a match between the empirical sphere echo and the gaussian mixture model.

Figure 3 shows positive identifications of the the steel sphere amongst the other targets at various ranges and orientations relative to the direction of deployment. The dolphin-inspired sonar image is given in the left image with the corresponding detection result on the right. In all cases the lower log-likelihood values indicate higher confidence in recognition. The resonant targets similar to the large steel sphere such as the small steel sphere or the PVC sphere are 10 dB higher in the log-likelihood

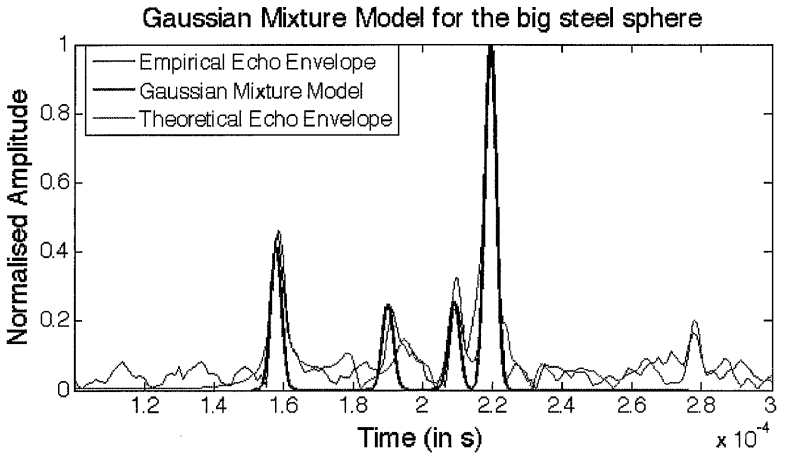

Figure 2: Time-frequency representation of the bio-inspired double chirp signals.

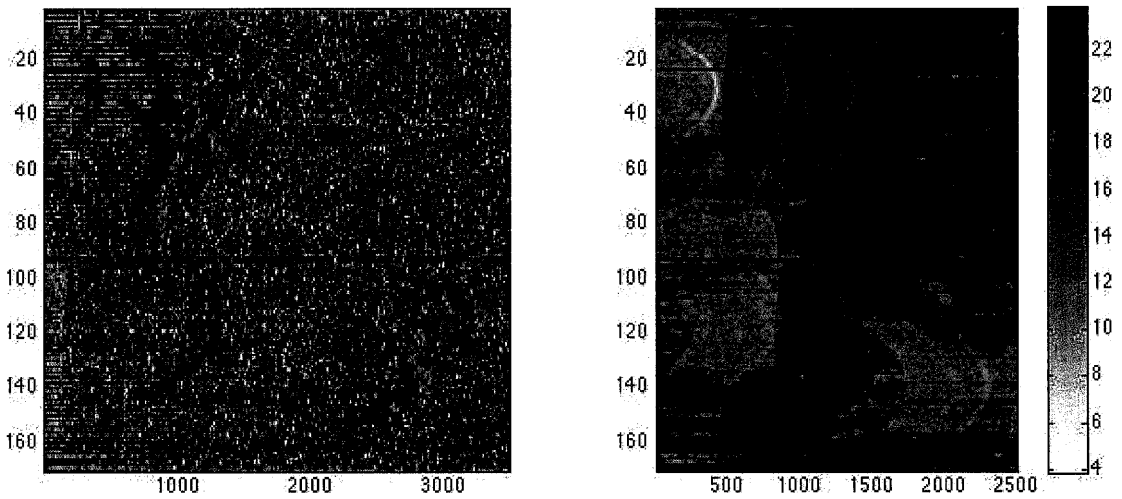

Figure 3: Left: BioSonar image of the target set. Right: Detection results.

feature and the background is 20 dB higher. These demonstrate correct object identification that is not possible with an image based system.

4 DOLPHIN LIKE REACQUISITION MISSION

Dolphins have been observed spiralling in on an object of interest, allowing them to gain views of the object from different angles. Here we describe some preliminary experiments where the results on object identification from an AUV are built upon using similar reacquisition strategies.

These trials again used a REMUS-100 autonomous underwater vehicle (AUV) carrying a side-looking wideband sonar payload in addition to the standard fit MarineSonics sidescan sonar. Two objects were put on the seafloor and the AUV returned to these objects and reacquired them following a dolphin-like spiral to obtain further data giving a range of views of the objects. The first object is a cylinder and the second object is a truncated cone shaped aluminium shell as shown in figure 4.

In this mission the reacquisition by the vehicle followed a two-turn octagonal spiral centred on the estimated position of each target of interest. The spirals start at 25 metres radius and finish after two full turns with a 20 metre radius. This track for the reacquisition is shown in figure 5. For these

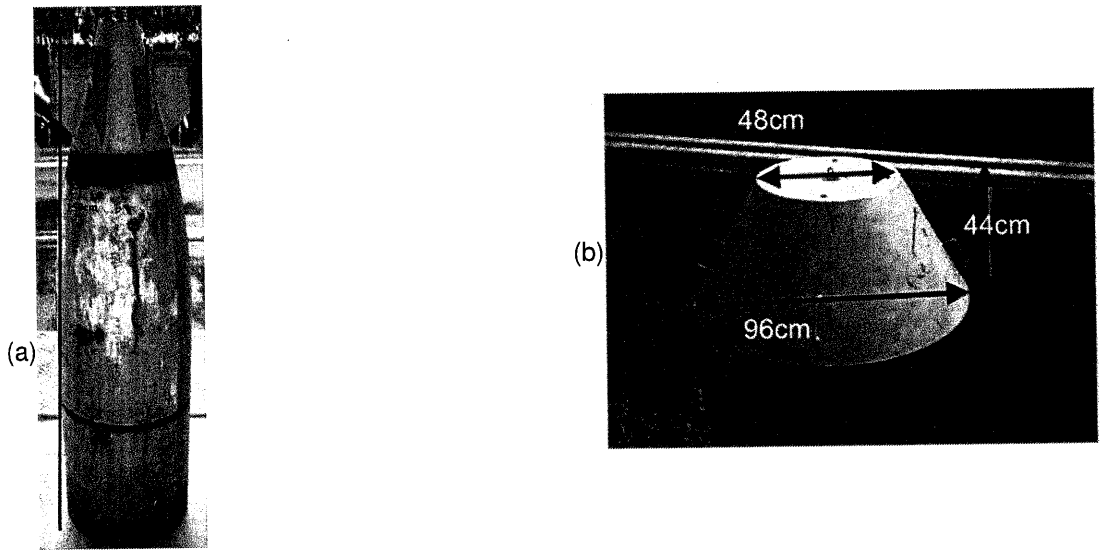

Figure 4: *(a)* Image of first object, *(b)* Image of second object.

reacquisition patterns, the wide beam of the BioSonar system is ideal and we can rapidly gather an almost continuous 720° acquisition giving a complete multiaspect description of these targets.

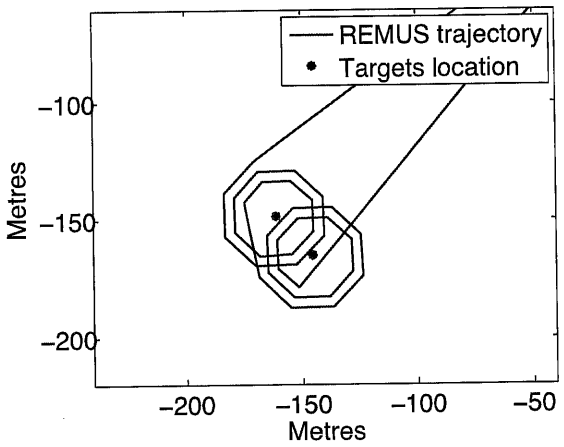

Figure 5: REMUS track of the reacquisition mission.

The returns from the BioSonar for one turn around the first cylindrical object are shown in figure 6(a). Figure 6(b) shows one single return from the BioSonar for the cylinder. In figure 6(a) the returns vary corresponding to the different aspects the object is being viewed from. It is this multi-aspect view which we use to be able to accurately identify both objects and their orientation. Each of the individual returns contains information on the object.

The returns from the BioSonar for one circuit of the second object, the truncated cone, are shown in figure 7(a). Figure 7(b) shows a single return from the BioSonar for the truncated cone. The returns seen in figure 7(a) are highly consistent over the whole circuit. This is because of the symmetrical nature of the target and again this gives important information for identification of the object.

These data supplied demonstrate the value of the wideband sonar system for identifying seafloor objects and show how the acquisition process can aid identification.

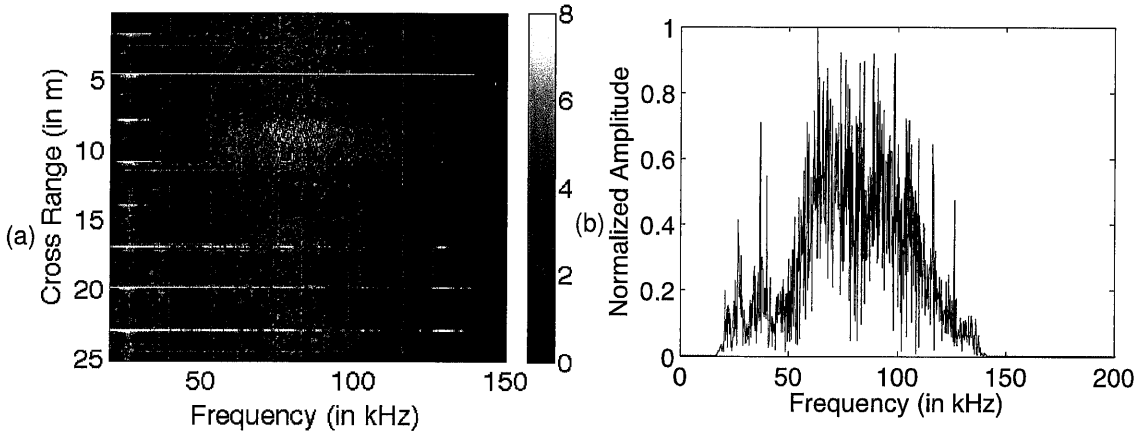

Figure 6: *(a)* BioSonar returns for cylinder, *(b)* Single BioSonar return for cylinder.

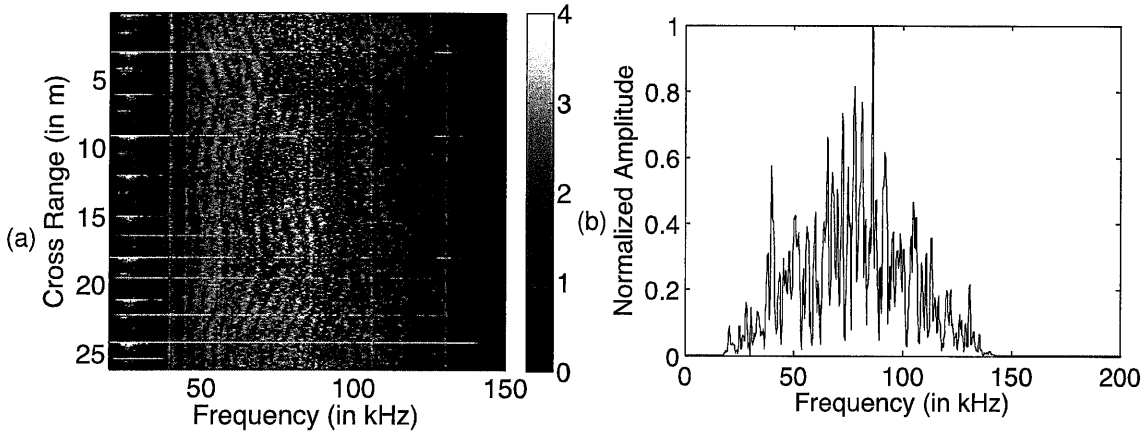

Figure 7: *(a)* BioSonar returns for truncated cone, *(b)* Single BioSonar return for truncated cone.

5 CONCLUSION

The dolphin-inspired sonar prototype described in this paper has been built based around the dolphins' sonar characteristics. Analyses have been presented to show the benefits that could be gained from using a dolphin-like sonar system. The operating frequency is lower than classical imaging sonars and because of the wide beamwidth, the sonar loses in resolution, compared to a conventional imaging system. However, this loss in resolution is compensated by the additional information provided by analysis of the full echo.

The capabilities of the system for object identification have been demonstrated. In a test tank the system has been shown to correctly discriminate between a set of six objects, with similar shapes and sonar responses, with a better than 90% success rate. The object identification has also been tested in open water experiments, where the system was able to correctly identify objects on the seafloor, in circumstances where the traditional sidescan sonar could only perform the simpler task of detection, not identification.

Further work is required to develop new algorithms, which will enable further exploitation of the information present in the sonar returns from the dolphin-inspired sonar. These new algorithms will support: increased probability of identification; reduced probability of false alarms; greater ranges of operation and the ability to deal more effectively with buried objects.

REFERENCES

1. J. J. Faran. Sound scattering by solid cylinders and spheres. *J. Acoust. Soc. Am.*, 23: pp. 405–418, 1951.

2. R. Hickling. Analysis of echoes from a solid elastic sphere in water. *J. Acoust. Soc. Am.*, 34: pp. 1582–1592, 1962.

3. R. Goodman and R. Stern. Reflection and transmission of sound by elastic spherical shells. *J. Acoust. Soc. Am.*, 34(3): pp. 338–344, 1962.

4. R. Doolittle and H. Uberall. Sound scattering by elastic cylindrical shells. *J. Acoust. Soc. Am.*, 39(2): pp. 272–275, 1966.

5. Y. Pailhas, C. Capus, K. Brown, and P. Moore. Analysis and classification of broadband echoes using bio-inspired dolphin pulses. *J. Acoust. Soc. Am.*, 127(6): pp. 3809–3820, 2010.

6. G. Gaunaurd and H. Uberall. RST analysis of monostatic and bistatic acoustic echoes from an elastic sphere. *J. Acoust. Soc. Am.*, 73(1): pp. 1–12, 1983.